CrossMark

Effect of detonation nanodiamond surface composition on physiological indicators of mitochondrial functions

Andrey S. Solomatin · Ruslan Y. Yakovlev · Vera V. Teplova ·
Nadezhda I. Fedotcheva · Mariya N. Kondrachova · Inna I. Kulakova ·
Nikolay B. Leonidov

Abstract For the first time, an effect of detonation nanodiamonds (NDs) with different surface compositions on the main functional characteristics of isolated rat liver mitochondria was studied. The response of membrane potential, calcium retention capacity, and redox state of pyridine nucleotides have been monitored upon the administration of NDs functionalized with carboxyl, hydroxyl, amine, hydrogen, and chlorine surface groups. Hydrogenated and chlorinated NDs caused reduction of the membrane potential and calcium retention capacity of mitochondria. An aminated ND caused an even greater decrease in calcium retention capacity (at a concentration of 0.75 mg/ml), reducing it to 65% of the control. The use of cyclosporine A prevented a decrease in membrane potential and calcium retention capacity indicating the induction of non-specific mito-chondrial membrane pores during the NDs incubation with mitochondria. Hydrogenated and chlorinated NDs had no significant effect on the redox state of mitochondrial pyridine nucleotides. Other NDs studied had no effects on functional characteristics of mitochondria, even at high concentrations (up to 1.5 mg/ml). High activity of chlorinated and hydrogenated NDs may be due to the greater hydrophobicity of their surface and its interaction with mitochondrial pores components. Thus, isolated rat liver mitochondria can be used as a biomodel for initial testing of ND samples to assess the possibility of their use in drug delivery systems.

A. S. Solomatin · R. Y. Yakovlev · N. B. Leonidov
Pavlov Ryazan State Medical University, Ryazan, Russia

A. S. Solomatin (✉) · I. I. Kulakova
Faculty of Chemistry, Lomonosov Moscow State University,
GSP-1, 1-3 Leninskiye Gory, Moscow 119991, Russia
e-mail: solo-msu@yandex.ru

R. Y. Yakovlev
Vernadsky Institute of Geochemistry and Analytical Chemistry of
the Russian Academy of Sciences, Moscow, Russia

V. V. Teplova · N. I. Fedotcheva · M. N. Kondrachova
Institute of Theoretical and Experimental Biophysics of the
Russian Academy of Sciences, Pushchino, Russia

Introduction

Currently, one of the main areas of modern nanomedicine, nanochemistry, biopharmaceutics, and pharmaceutical nanotechnology is the development of delivery systems of biologically active substances (BAS) and drugs based on a variety of nanoparticles to improve the efficiency of treatment and to reduce toxicity and possible adverse events (Balogh 2017; Pathak and Thassu 2016).

Springer

Among more than over 400 kinds proposed nanoparticles, one of the most promising nanocarriers are carbon nanostructures, including single-wall and multi-walled carbon nanotubes, fullerenes, graphene and its oxide, and nanodiamonds (Mendes et al. 2013; Wong et al. 2013; Hong et al. 2015; Shenderova and Gruen 2006; Ho et al. 2015; Chen and Zhang 2017). The attractiveness of carbon nanocarriers is due to ample opportunities of overcoming biological barriers, penetration into cells, immobilization of different BAS, and drugs and their different combinations (Mendes et al. 2013). However, several studies have found significant differences in the biological properties of these nanostructures, including toxicity (Wong et al. 2013; Hong et al. 2015; Shenderova and Gruen 2006; Ho et al. 2015). It is shown that one of the least toxic members of nanocarbon family is ND (Hong et al. 2015; Ho et al. 2015).

Detonation nanodiamond (ND) is characterized by an optimal combination of advantageous characteristics namely the small primary particle size (4–6 nm), rounded shape, high-specific surface area (~ 400 m^2/g), and the presence of a variety of functional groups on the surface (Magrez et al. 2006; Jia et al. 2005; Danilenko 2004; Dolmatov 2007). Furthermore, it was found that the ND is able to penetrate the blood-brain barrier (Zhang et al. 2012). High concentrations of various functional groups on the surface of ND allow specific functionalization of the ND surface chemistry for its binding with BAS and drug molecules (Shugalei et al. 2013; Yakovlev et al. 2014). Many studies have indicated that variations in the composition of surface functional groups are often accompanied by changes in the biological properties of the carbon nanoparticles. This is true both for fullerene (Sayes et al. 2004) and carbon nanotubes (Sayes et al. 2004, Bottini et al. 2006), as well as for NDs (Weng et al. 2012; Wehling et al. 2014; Whitlow et al. 2017).

Application of nanodiamonds (NDs) in the biomedical fields requires a thorough study not only of their chemical and physicochemical characteristics, but also biological, pharmacological, and toxicological properties, including their influence on cellular and subcellular levels of the organism.

It was revealed (Schrand et al. 2007) that NDs penetrate into neuroblastoma cells and macrophages, and are localized in the cytoplasm to form aggregates of about 500 nm. This ND with oxidized surface does not lead to increased levels of reactive oxygen species (ROS). Several other studies also confirmed

penetration of NDs in various cells: HeLa (Mkandawire et al. 2009), neutrophils (Karpukhin et al. 2011), mouse macrophages (Thomas et al. 2012), platelets (Kumari et al. 2013), human peripheral lymphocytes (Dworak et al. 2014), and a variety of other cell lines (Zhang et al. 2012; Yakovlev et al. 2014; Weng et al. 2012; Wehling et al. 2014; Whitlow et al. 2017). It has been shown that NDs' localization in cells can be both on the surface of the cell membrane and in the cytoplasm (Schrand et al. 2007; Karpukhin et al. 2011), including the nuclear region and intracellular organelles, such as mitochondria (Mkandawire et al. 2009; Chan et al. 2017). As mitochondria are the central component in the chain of energy metabolism of cells (Munnich and Rustin 2001), disruption of normal mitochondria functioning can lead to the development of cell pathologies, the emergence of a number of severe diseases and even the death of the organism (Halliwell 1991; Cheung et al. 2017). Mitochondria are also the major source of ROS, which, with mitochondrial dysfunction, may increase the destruction and even death of cells (Turrens, 2003). A number of studies have been shown to cause mitochondrial dysfunction could be nanoparticles of different nature: silica (Guo et al. 2018), quantum dots (Zheng et al. 2017) et al. (Zhao et al. 2016; Naserzadeh et al. 2018), including NDs (Mytych et al. 2016; Fresta et al. 2018).

While some studies (Kumari et al. 2013, Dworak et al. 2014) report that the ND concentration of about 1–5 μg/ml in the incubation medium creates noticeable changes in the normal state of the cells, such as increased ROS and reduced cell viability, according to other studies (Sayes et al. 2004; Wehling et al. 2014; Schrand et al. 2007), the adverse effects occur at much higher ND concentrations (> 50–100 μg/ml). This mismatch of the results from experimental studies of biological activity of NDs can be attributed both to the use of various cell cultures and the conditions of incubation, as well as the difference in the nature of the composition of impurities (Mitev et al. 2014) and functional groups on ND surface (Korolkov et al. 2007). Thus, the qualitative and quantitative composition of impurities, in particular, metals with variable valence can greatly affect the results of the biological action of NDs (Mitev et al. 2014). It has also been shown that the effect of nanostructures on the mitochondria can significantly depend on the particle size (Lai et al. 2016).

Based on the results published, we can conclude that the NDs, similar to some therapeutic substances (Szewczyk and Wojtczak, 2002), after penetrating into cells, may be capable of acting on mitochondrial function and consequently on metabolism of cells. One of the most important indicators of mitochondria functioning is maintaining certain value of the membrane potential; otherwise, the sustaining of the normal functioning of mitochondria is sustained (Chen 1988). The ratio of the oxidized and reduced forms of coenzyme nicotinamide adenine dinucleotide (NAD) (i.e., $NAD^+/NADH$) or dynamics of its change in the process of oxidative phosphorylation can be used as an indicator of the metabolic activity of mitochondria (Schafer and Buettner 2001). Another important indicator of the state of mitochondria is their ability to transport and accumulate calcium ions, which performs regulatory and signaling functions in mitochondria and cells (Babcock et al. 1997; Cheung et al. 2017). The impairment of the ability of mitochondria to absorb calcium ions can lead to the dysfunction of mitochondria and cells death (Nutt et al. 2002).

Up to now, the effect of the ND's surface on mitochondrial functions has not been sufficiently investigated. Therefore, the aim of this work is a complex study of the effect of ND's surface composition on such characteristics of mitochondrial functioning as the membrane potential, calcium retention capacity, and redox state of pyridine nucleotides.

Experimental

Nanodiamond

In the present study, ND (trade mark UDA-TAN) from the company "SCTB "Technolog", St. Petersburg, Russia was used. This sample contained 0.7 wt% of non-combustible impurities. To reduce the content of metals and other impurities, the ND was sequentially treated with 0.1 M NaOH solution and concentrated HCl. After every treatment, the ND was thoroughly washed with water and dried using a rotary evaporator.

Next, this purified ND sample (ND(ref)) was used to obtain functionalized samples of ND.

Hydrogenation

The nanodiamond with hydrogen-containing surface groups (ND-H) was prepared by thermal gaseous hydrogenation, as described in the article (Karpukhin et al. 2011). A quartz reactor with the ND(ref) sample was placed in a tube furnace, heated to 800 °C and held for 5 h in a stream of hydrogen (at 2–3 l/h flow rate).

Chlorination

The ND with chlorinated surface groups (ND-Cl) was prepared as described in the article (Lisichkin et al. 2006). Chlorine was prepared by reacting $KMnO_4$ with concentrated HCl; the liberated gas was absorbed by carbon tetrachloride until its saturation (at 5.6 wt%). ND-H (500 mg) was added to 40 ml of CCl_4 and Cl_2, and the mixture was kept under an incandescent lamp (500 W) at constant stirring for 24 h. Then, the ND-Cl was separated from the solution, rinsed with CCl_4, dried using a rotary evaporator, and degassed under vacuum (< 1 bar) for 2 h. The ND-Cl was stored in a desiccator over calcium chloride.

Amination

Aminated nanodiamonds (ND-NH_2) were prepared by a thermal gas-phase amination of ND-Cl (Denisov et al. 2010). 0.5 g of ND-Cl was placed in a quartz boat and transferred to a tubular furnace. Then, it was treated with ammonia (2–3 l/h) at 450 °C for 1 h. The ND-NH_2 was degassed under vacuum (< 1 bar) for 2 h.

Carboxylation

Carboxylated ND (ND-COOH) was prepared through liquid-phase oxidation of ND(ref) with a mixture of acids, by a method similar to that described in previous work (Nebel et al. 2007). One gram of ND(ref), placed in a glass flask equipped with a reflux condenser, was treated with 50 mL of a boiling mixture of concentrated acids HNO_3: H_2SO_4 (1: 3) for 24 h. After separation of ND-COOH ND from the acids, the ND was treated twice with 50 ml of 0.1 M NaOH solution and once with 50 ml of 0.1 M HCl solution. ND-COOH was washed with water and dried using a rotary evaporator for 2 h, then degassed under vacuum (< 1 bar) for 2 h.

Hydroxylation

Hydroxylated ND (ND-OH) was prepared by reduction of ND-COOH according to the procedure described in (Hens et al. 2008). A sample weight of ND-COOH (1 g)

was placed in a three-necked round flask and 10 ml of anhydrous degassed tetrahydrofuran (THF) and 15 ml of 2 M LiAlH$_4$ solution in THF were added. The reaction mixture was stirred under nitrogen for 12 h. Residue of LiAlH$_4$ was decomposed with 1 M HCl. ND-OH suspension was washed successively with 1 M HCl and distilled water. Washed ND-OH was dried using a rotary evaporator for 2 h and degassed under vacuum (< 1 bar) for 2 h.

All NDs' functionalization steps are shown in Fig. 1.

Preparation of ND hydrosols

Biological tests of ND influence on the functional characteristics of mitochondria were performed using hydrosols of ND(ref) and functionalized NDs. Preparation of these hydrosols was done by the method described in the previous work (Yakovlev et al. 2015). A sample of NDs (500 mg) was added to a test tube with 10 ml of Milli-Q water and dispersed by sonication (250 W/cm^2) for 1 min. Large particle of NDs were removed by centrifugation ($\times$ 6000g) for 5 min. Immediately before performing the experiment with the mitochondria, the pH of hydrosols prepared with NDs was adjusted to 7.2–7.4 using a 1 M solution of KOH.

Characterization of NDs

Electron microscopic images of ND particles were obtained with an ultra-high resolution transmission electron microscope, JEM-2100 F ("JEOL," Japan) with 2 Å resolution.

Before registration of the FTIR-spectra, the ND sample was dried at 100 °C under a pressure < 1 bar for 2 h. The absorption spectra of NDs were recorded using tablets made of KBr (in the same weight ratio of KBr and ND and identical tablets weight for all samples) on the Nicolet IR200 FTIR spectrometer ("Thermo Scientific," USA). The measuring range is 400–4000 cm^{-1}, resolution 2 cm^{-1}, 50 scans. The software EZ Omnic (ACDLabs 10, Canada) was used for the data analysis. Selected shooting conditions of the IR spectra allowed semi-quantitative evaluation of changes in the functional groups on the surface of the NDs.

The chemical composition of the NDs surface was analyzed by XPS spectrometer LAS-3000 ("Riber," France) equipped with a hemispherical analyzer OPX-150. For the excitation of the photoelectrons, the non-monochromatic X-ray radiation from aluminum anode (AlKα = 1486.6 eV) was used at the tube voltage of 12 kV and emission current of 20 mA. The vacuum in the chamber was 5×10^{-10} Torr. The calibration of photoelectron peaks was performed relatively to the carbon C 1 s peak with binding energy (E_b) 285 eV.

The determination of carbon, hydrogen, and nitrogen in NDs was performed using a combustion analyzer 240G ("Perkin Elmer", USA). The ND sample (3–6 mg) was placed in a platinum boat in the analyzer. Combustion was conducted in a stream of pure oxygen at 950 °C for 20 min. The content of CO$_2$, H$_2$O, and N$_2$ in the combustion products was determined chromatographically. From the difference in the initial sample weight and content of C, H, and N, the total weight of incombustible residue and oxygen was calculated.

The determination of chlorine in the ND samples was performed by their combustion and subsequent absorption of product gas by silver flakes at 440–445 °C that is 15 °C below the melting point of silver chloride, and the increase in weight of silver provided the chlorine content. According to the weight of the

Fig. 1 Stages of ND(ref) functionalization:
1—carboxylation,
2—hydroxylation,
3—hydrogenation,
4—chlorination, 5—amination
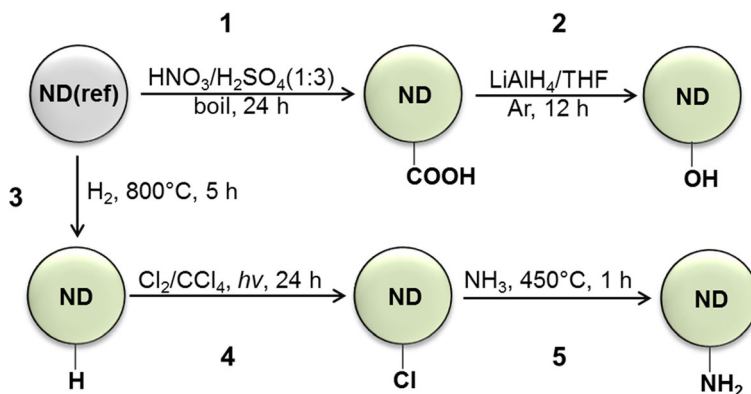
noncombustible residue, oxygen content in the ND sample was calculated.

Characterization of ND hydrosols

The concentration of NDs in hydrosols was determined by weighting the sample before and after evaporation of water from 0.5 ml of a ND hydrosol heated to 200 °C. Hydrodynamic diameter of the NDs in hydrosol was determined by dynamic light scattering (DLS) technique using the ZetaSizer Nano ZS analyzer (Red Badge—633 nm) and ZEN 3600 (Malvern instruments, LTD, USA). The hydrosols were diluted to a concentration of 0.5 mg/ml.

In vitro studies

Animals

The study used adult male rats of the Wistar variety (vivarium ITEB RAS, Pushchino, Russia), weighing 230–250 g (We worked in full compliance with the European Convention for the Protection of Vertebrate Animals Used for Experimentation and other Scientific Purposes, 1986 86/609/EEC.).

Isolation of rat liver mitochondria

Rat liver mitochondria (RLM) were isolated from rat liver according to standard procedures (Johnson and Lardy 1967). After decapitation of the animal, livers were removed and homogenized in a cooled extraction medium containing 300 mM sucrose, 10 mM tris(hydroxymethyl)aminomethane (Tris-HCl) (pH 7.4). The homogenate was centrifuged at 1800g-forces for 6 min at 0 °C. The supernatant was separated and centrifuged at × 5000g-forces for 20 min at 0 °C. The mitochondrial precipitate was resuspended in the extraction media. The mitochondrial suspension was kept on ice. Protein content was determined by the Biuret method using bovine serum albumin as a standard (Gornall et al. 1949).

Measurements of the mitochondrial membrane potential in isolated mitochondria (in vitro)

For determination of mitochondrial membrane potential, we used the method described in the article (Kondrashova et al. 2001). All measurements were performed with continuous stirring in a thermostatic cuvette with a volume of 1 ml at 25 °C. Potassium succinate, with the addition of rotenone and potassium pyruvate, was used as an oxidation substrate. Mitochondrial membrane potential was determined by the distribution of the lipophilic cation tetraphenyl phosphonium (TPP^+), whose concentration in the incubation medium was recorded with the help of TPP^+-selective electrode by the computerized system Record 4 (ITEB RAS, Russia) (Kamo et al. 1979). The results are reported as the concentration of TPP^+ in the incubation medium on time.

Mitochondria (20 μl; 1.2 mg of protein) was incubated in 1 ml of medium containing 120 mM KCl, 1.5 mM KH_2PO_4, 10 mM 4-(2-hydroxyethyl)-1-piperazineethanesulfonic acid (HEPES) (pH 7.25), 4 mM of substrate oxidation, and 1 μM TPP^+. We used pyruvate potassium or complex of succinate potassium with rotenone as oxidation substrates. All measurements were performed in a thermostated 1-ml cuvette at 25 °C with continuous stirring. In each experiment, 10 μl of ND hydrosol (i.e., 500 μg ND) were added to the media starting at the 100th second and then every 60 s for five times in total. Three independent experiments per data point were conducted.

Determination of the calcium retention capacity of isolated mitochondria

Calcium RLM capacitance measurement was performed according to the procedure described in (Kondrashova et al. 2001). Measurements were carried out under continuous stirring in a thermostatic cuvette with its volume of 1 ml at 25 °C using a Ca^{2+}-selective electrode and computerized system Record 4 (RAS ITEB, Russia) (Fedotcheva et al. 2009). A mixture of potassium glutamate (4 mM) with potassium malate (2 mM) was used as the oxidation media. An oxidation substrate and RLM (20 μl; 1.2 mg of protein) in 1 ml medium were added to the incubation medium, followed by addition 15 or 30 μl of ND hydrosols (i.e., 0.75 or 1.5 mg ND). Sequential addition of 25 μM $CaCl_2$ was added until the recorded calcium ion concentration stopped to be accumulated in mitochondria. Calcium retention capacity was determined by the amount of accumulated Ca^{2+}. The measurement results are presented as the time-dependent concentration of Ca^{2+} (μM) in the incubation medium.

Evaluation of redox state of pyridine nucleotide and oxidative phosphorylation of isolated mitochondria

Redox state of pyridine nucleotide and oxidative phosphorylation of isolated mitochondria was assessed by fluorescence of pyridine nucleotides (at 460 nm) at an excitation wavelength of 340 nm in a suspension of mitochondria using the Hitachi-F700 fluorimeter (Japan). To the measuring cuvette with incubation medium (125 mM KCl, 15 mM HEPES, 1.5 mM phosphate, pH 7.25), the oxidation substrate (mixture of glutamate and malate potassium at 5 mM) and 20 μL of mitochondria (0.6 mg of protein per ml) were added, followed by the addition of 25 μl of the ND hydrosol. To evaluate oxidative phosphorylation, 200, 400, and 800 μM of adenosine diphosphate (ADP) were added. Complete oxidation of NADH was induced by adding 0.5 μM of uncoupler carbonyl cyanide-4-(trifluoromethoxy)phenylhydrazone (FCCP).

Results

Physicochemical characterization of samples of NDs and hydrosols

The specific surface area of ND was determined by the Bruner–Emmett–Teller (BET) method from the data on the low temperature adsorption of nitrogen on the Gimini 2390 V1/02t instrument (Micromeritics, USA), and it was equal to 296 ± 1 m^2/g. As it can be seen from the TEMHR-micrographs of ND particles (Fig. 2), the diamond core of the nanoparticles is clearly visible. The
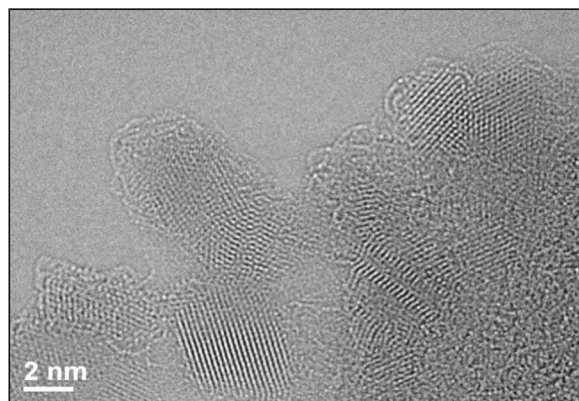
Fig. 2 TEMHR image of the ND(ref)

primary particle size averages 5–6 nm, which corresponds to the in literature data (Kulakova 2004). A similar pattern is typical for all studied NDs.

Figure 3 shows the absorption spectra obtained by FTIR-samples of NDs. In all FTIR-absorption spectra of the ND samples (Fig. 3), a broad intense band with the maximum at 3435 cm^{-1} is observed that is due to the presence of oxygen-hydrogen bonds of hydroxyl groups and adsorbed water molecules on the surface of ND. The stretching valence vibrations of CH-groups correspond to 2928 and 2856 cm^{-1}. The absorption band with the maximum at 1726 cm^{-1} is due to the presence of carbonyl groups on the ND surface. The absorbance at 1631 cm^{-1} is connected with the bending vibrations of water molecules adsorbed on surface NDs.

The disappearance of absorption bands at 1726 cm^{-1}, characteristic for the spectrum of the ND(ref) is observed (line a) and Fig. 3 demonstrates that in the spectrum of the sample ND-H (line b). Simultaneously, there is an increase in intensity of the band corresponding to oscillations of C-H-bonds at 2928 cm^{-1} and a shift of the band from 2856 cm^{-1} to 2885 cm^{-1}. The samples of ND-Cl and ND-NH$_2$ (lines c-d) were almost identical. The spectra of ND-COOH and ND-OH samples (lines e–f) preserved the absorption band of the carbonyl group. In case of ND-COOH, its relative intensity compared with that of pure ND increased. In the spectra of samples of ND-COOH and ND-OH at 1120 cm^{-1}, stretching vibrations also manifest ether bonds (C-O-C), which are more intense than those observed in the spectrum of the starting ND (line a). After treatment of ND-COOH sample with a reducing agent (LiAlH$_4$), the intensity of the absorption band corresponding to the vibrations of the carbonyl groups is significantly reduced, which means the reduction in the amount of carboxyl groups on the surface of nanoparticles (line g). The bands in the region 1400–1000 cm^{-1} can be attributed to the intrinsic absorption of the diamond lattice (Kulakova 2004).

The composition of the surface layer of ND particles, obtained from XPS analysis, is shown in Table 1.

The data in Table 1 show that oxygen content varies from 2.6 at% in ND-H to 7.5 at% in ND-COOH. The same amount of nitrogen was observed in almost all samples, except NDs ND-NH$_2$ functionalized, where it was higher (~ 1.9 at%). At the same time, in all other samples, minor amount of chlorine was also observed. This may be due to the presence of impurities of metal chlorides. Indeed, in the Cl2p XPS-spectrum of the

Fig. 3 FTIR-absorption spectra of the NDs studied. The rectangles show the areas of the spectrum in which the most significant changes are observed in the process of surface functionalization of ND
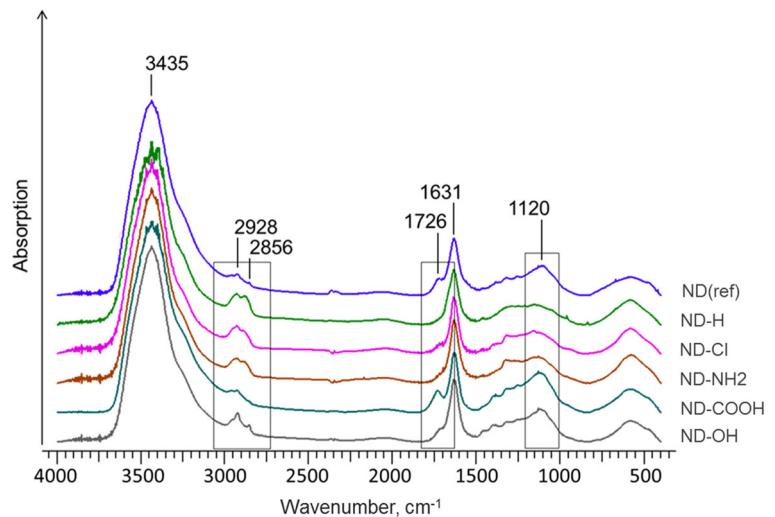
ND(ref) sample, a peak corresponding to chlorine in the form of chloride anions (196.5 eV) was present, while the spectrum of the ND-Cl sample contained the peak at around 200 eV, corresponding to chlorine covalently bound with the surface carbon atoms (Fig. 4).

The results of elemental analysis of NDs, obtained by combustion analysis, are summarized in Table 2.

Despite the fact that the main method for analyzing the chemical composition of the surface is XPS, Table 2 lists some ND samples. The analysis of samples by the combustion method additionally makes it possible to determine the hydrogen content, which makes it possible to control the qualitative modification of the surface in the chain "ND(ref) – ND-H – HA-Cl." Therefore, data only for these three samples are presented.

Table 2 demonstrates that nitrogen content is the same in different samples of NDs. Oxygen content in

samples of ND-H and ND-Cl is nearly twice as lower as in that of ND(ref). Simultaneously, hydrogen content in the ND-H is twice as higher as in ND(ref). The chlorine content in ND-Cl sample is significantly higher than that in ND(ref) sample indicating the covalent grafting of chlorine to the ND surface.

Parameters of ND hydrosols studied

According to DLS data, the average hydrodynamic diameter of particles in hydrosols of functionalized NDs ranged from 150 to 200 ± 10 nm (Table 3).

Table 4 provides pH ranges from 3 to 4 for the majority of the samples (except hydrosols of ND-H and ND-NH$_2$), indicating acidic character of the samples (at 50 mg/ml). Considerably higher, pH of hydrosols ND-H and ND-NH$_2$ samples apparently reflects a reduced content of proton-donating groups on the surface of both ND samples. Another contribution to the higher pH of the hydrosol of the sample ND-NH$_2$ may be due to amino groups located on its surface, which have a weakly basic nature.

Table 1 Content of elements in the surface layer of the ND particles, according to XPS analysis

Sample	Content of elements, at% (normalized to C, O, N, and Cl)*			
	C	N	O	Cl
ND(ref)	92.7	1.5	5.5	0.3
ND-H	95.6	1.5	2.6	0.3
ND-Cl	95.1	1.5	2.7	0.7
ND-NH$_2$	93.9	1.9	4.1	0.1
ND-COOH	91.2	1.1	7.5	0.2
ND-OH	92.8	1.5	5.4	0.3

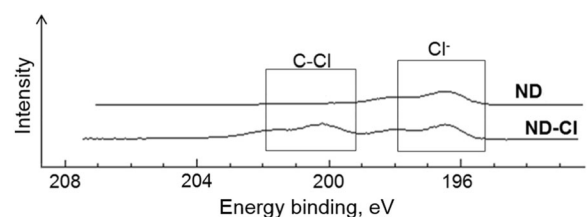*Accuracy of the method is ± 0.3 at%

Fig. 4 XPS-spectra of Cl2p-electrons of ND(ref) and ND-Cl

Table 2 The main elemental composition of ND samples obtained by combustion analysis

Sample	Amount of incombustible residue, wt%	Element content, wt%*				
		C	N	O	Cl	H
ND(ref)	0.7	89.7	2.3	6.7	<0.3	0.4
ND-H	1.3	91.2	2.3	3.7	0.7	0.8
ND-Cl	0.4	89.7	2.3	3.8	3.2	0.6

*Accuracy of the method is ± 0.3 wt%

Influence of functionalized NDs on mitochondrial membrane potential

Changes of mitochondrial membrane potential with various additives of NDs is shown in Fig. 5.

From Fig. 5a, it is seen that during normal functioning the mitochondria absorb positively charged lipophilic cation tetraphenyl phosphonium (TPP$^+$), due to the high values of the membrane potential. This leads to a decrease in the indicator concentration in the environment, where measurements were conducted. In the control experiment, the concentration of TPP$^+$ in the environment medium is maintained at a constant minimum level for more than 600 s (Fig. 5a, curve 1). The addition of most of functionalized NDs leads to increasing the concentration of TPP$^+$ in the environment medium, as a result of its leaving from the mitochondria, while decreasing mitochondrial membrane potential (Fig. 5a, curves 2 and 3). It is found that all ND samples with a modified surface reduce the membrane potential by acting at various concentrations. The greatest decrease in mitochondrial membrane potential was achieved with additions of ND-Cl and ND-H and the smallest at additives unmodified ND and ND-COOH (Fig. 5b).

Table 3 The values of average hydrodynamic diameter of studied ND particles in their hydrosols (0.5 mg/ml), according to DLS

ND samples	The average particle hydrodynamic diameter ND, nm
ND(ref)	178
ND-H	182
ND-Cl	154
ND-COOH	203
ND-OH	148
ND-NH$_2$	154

Since the presence of impurities (especially metals with variable valence) can substantially change the biological properties of the NDs (Keremidarska et al. 2014), a control experiment using additionally purified ND and ethylenediaminetetraacetic acid (EDTA) for removal of residual metal ions was performed. However, no changes of the ND activity were observed, which means the absence of any metal impurities in the investigated nanodiamond.

It was found that the decrease in mitochondrial membrane potential induced by samples of NDs was prevented by adding a known inhibitor of mitochondrial non-specific pores (mitochondrial permeability transition pore, MPTP) cyclosporine A (CsA). In Fig. 6, as an example, the effect of CsA on the changes of mitochondrial membrane potential caused by supplements ND-Cl is presented (curve 1). It was discovered that CsA not only prevents the reduction of mitochondrial membrane potential induced additions of ND-Cl (Fig. 6, curve 3) but also restores it even after a significant reduction (Fig. 6, curve 2).

Influence of the ND surface chemistry on the transport of calcium ions and calcium retention capacity of isolated mitochondria

The results of experiments on studying of influence of chemical composition of NDs surface on the transport of calcium ions and the calcium retention capacity of mitochondria are shown in Fig. 7.

As can be seen from the figure, the addition of the hydrosol ND-Cl and ND-H to isolated mitochondria causes a decrease in calcium retention capacity, depending on the amount of hydrosol added (Fig. 7a, b). Adding of 0.75 mg/ml of hydrosols of ND-Cl, the release of calcium from the mitochondria occurs at the fifth addition of 25 μM CaCl$_2$ and ND-H at the sixth addition of 25 μM CaCl$_2$. Adding of hydrosols in the

Table 4 Starting pH of NDs hydrosols (C = 50 mg/ml)

ND Sample	ND(pure)	ND-H	ND-Cl	ND-NH$_2$	ND-COOH	ND-OH
pH	4.1	6.9	3.2	5.0	3.5	3.3

amount of 1.5 mg/ml, the release of calcium from mitochondria occurs on the fourth additive as for ND-Cl and ND-H, while in the control mitochondria retain calcium even after 8–9 additives CaCl$_2$. Comparison of the action of all ND samples investigated on calcium retention capacity of mitochondria (Fig. 7c) showed that in the case of the original sample ND, the amount of calcium absorbed by mitochondria remains at the level of the control. The addition of ND-COOH and ND-OH hydrosols results to a weak decrease in the calcium retention capacity of mitochondria (only 10% of control) when the amount of ND suspensions, introduced into the cell, is 1.5 mg/ml. The addition of 0.75 mg/ml of hydrosols of samples ND-H, ND-Cl, and ND-NH$_2$ to the mitochondria reduces in the number of calcium trapped by mitochondria to 75 and 65% of control values, respectively (data not shown).

The increase in the concentration of the added hydrosol of samples ND-H, ND-Cl, and ND-NH$_2$ up to 1.5 mg/ml decreases the amount of calcium absorbed by mitochondria to 65 and 55% of control values, respectively (Fig. 7c).

Influence of NDs on redox state of pyridine nucleotides of isolated mitochondria

The observed change of the calcium retention capacity of mitochondria may be due to the effect of modified NDs to the redox state of the pyridine nucleotides in isolated mitochondria.

Figure 8 presents data on the effect of NDs on the redox state of the pyridine nucleotides in isolated mitochondria, which was assessed by changes in fluorescence of NADH in response to the addition of adenosine diphosphate (ADP) and disconnector, carbonyl cyanide-4-(trifluoromethoxy)phenylhydrazone (FCCP).

The additives of NDs were made at a concentration of 20 mg/ml. Mitochondria (0.6 mg protein) were added to 1 ml of incubation medium containing 120 mM KCl, 1.5 mM KH$_2$PO$_4$, 10 mM HEPES (pH 7.2), and oxidation substrate of 5 mM glutamate +5 mM malate (in the experiments presented in Fig. 8a) or 4 mM pyruvate + 2 mM malate (in the experiments presented in Fig. 8b).

The original recording of ND-NH$_2$ actions on change of the fluorescence of PN and cycle of oxidative
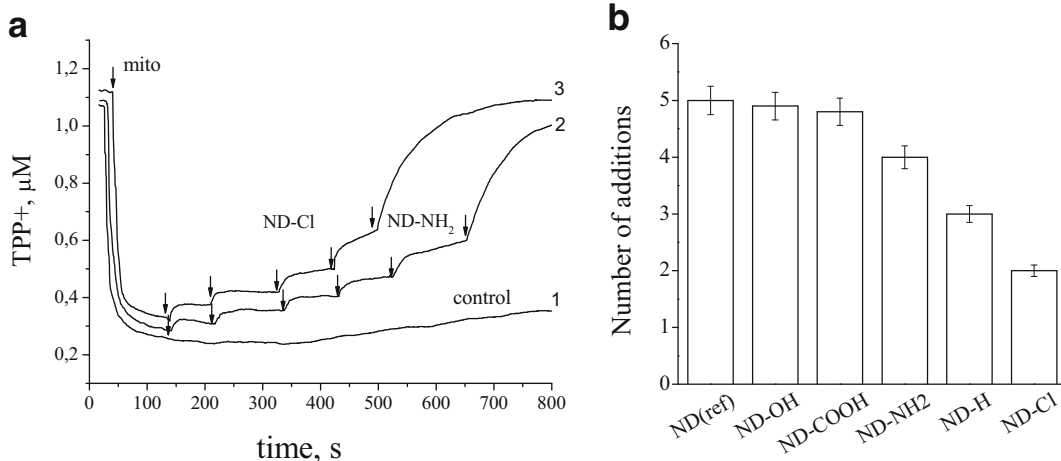
Fig. 5 The effect of functionalized NDs on mitochondrial membrane potential (as measured by changes in the concentration of TPP$^+$ in the environment, where measurements were conducted). **a** Original recording of changes in membrane potential of mitochondria, oxidizing pyruvate in control, no additive of ND (curve 1) and with consistent supplements of ND-H (curve 2) and ND-Cl (curve 3). The arrows mark the addition of a 10 µl hydrosol of ND (500 µg ND). **b** The number of functionalized ND hydrosols supplements (50 mg/ml) required to reduce mitochondrial membrane potential by 50%. The concentration of the components of the mixture in the measurement cell: 1.2 mg protein was added to 1 ml of incubation medium containing 120 mM KCl, 1.5 mM KH$_2$PO$_4$, 10 mM HEPES (pH 7.2), 4 mM substrate, and 1.2 µm TPP$^+$. The mixture was incubated at 25 °C
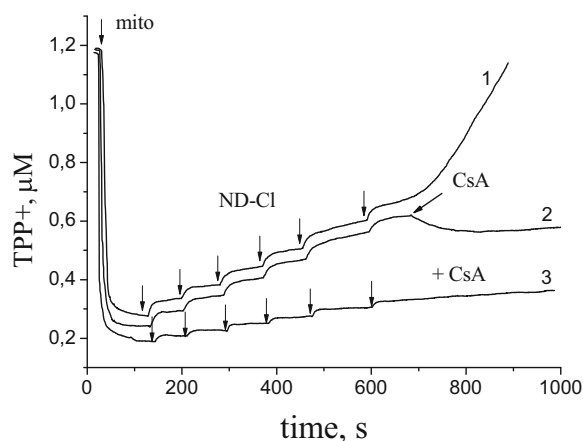
Fig. 6 Prevention by cyclosporine A reduction effect of the membrane potential induced by sample ND-Cl. 1—the mitochondrial potential change under the action of the sequential additives of the ND-Cl (500 μg), indicated by arrows; 2—cyclosporine A (2 μM) was added after the introduction of the ND-Cl; 3—cyclosporine A (2 μM) was added before the introduction of the ND-Cl. The concentration of the components of the mixture in the measurement cell: 1.2 mg protein in 1 ml of incubation medium containing 120 mM KCl, 1.5 mM KH_2PO_4, 10 mM HEPES (pH 7.2), 4 mM substrate oxidation (succinate), and 1.3 μM TPP^+. The mixture was incubated at 25 °C

phosphorylation of added ADP is shown in Fig. 8a as an example. It was found that ND-NH_2 sample was extinguished the initial fluorescence of pyridine nucleotides, but did not cause oxidation of NADH, as significant changes of oxidative phosphorylation (synthesis of ATP in response to ADP addition) and response to the addition of disconnector (FCCP) were not observed.

In assessing, the impact of modified NDs to the cycle time of oxidative phosphorylation was found that the majority of the studied NDs does not affect the cycle of oxidative phosphorylation to be determined in response to mitochondrial membrane potential to ADP addition. The estimate of modified NDs impact to the cycle time of oxidative phosphorylation allowed us to establish that most of the NDs does not affect the cycle of oxidative phosphorylation to be determined in response to mitochondrial membrane potential to ADP addition. However, the ND-Cl and ND-H caused the disconnection and lengthening of the oxidative phosphorylation time to 50% (Fig. 8b). In addition, it should be noted that current concentrations of ND-Cl and ND-H is sufficiently high (100–200 μg/ml), i.e., close to the concentrations that affect mitochondrial membrane potential in the absence of ADP.

Discussion

The analysis of TEMHR image of the studied NDs did not reveal any significant differences between the samples. TEMHR analysis demonstrates that NDs particles are spherical in shape; they have a well-formed diamond core, narrow particle size distribution, and the average particle size is in the range of 4–6 nm.

FTIR spectroscopy and XPS analysis emphasized the changes in the chemical composition of different NDs induced by surface modification (see Fig. 3 and Table 1). In particular, based on the reduction in the intensity of the absorption band of the carbonyl group (1726 cm^{-1}), FTIR spectrum analysis confirms the reduction of various oxygen-containing groups rather than hydroxyl (Jakovlev et al. 2013). Increase in the relative intensity of the absorption bands in the 2800–3000 cm^{-1} region indicates that the amount of C-H bonds on the surface of the ND-H sample increased. There was no a significant difference observed in the FTIR-spectra of the ND-H and ND-Cl samples (Fig. 3, lines b–c), since the absorption intensity of the C-Cl bonds is very low (Lisichkin et al. 2006).

There are also no differences in the FTIR-spectra of the ND-H and ND-NH_2 samples (Fig. 3, lines b–d). This is due to the fact that the absorption by amino groups manifested in a broad peak 3000–3500 cm^{-1} overlaps with the absorption by OH groups of water molecules adsorbed on ND-H surface through hydrogen interactions.

Changes in the relative intensity of the absorption band of C=O bonds (1726 cm^{-1}) indicates the quantitative difference between these bonds at the surface of the samples ND. Thus, in the case of ND-COOH, C=O bonds on the surface as compared to ND(ref) increases, and compared to ND-OH sample decreases.

Increased levels of oxygen in the ND-NH_2 sample compared with ND-Cl, from which it was derived, may be due to partial hydrolysis of the C-Cl on the surface of ND-Cl (Lisichkin et al. 2009) due to the presence of traces of water in ammonia in the amination process of ND-Cl (Table 1). Total nitrogen content of NDs (Table 1) does not change during the functionalization of the surface, which is consistent with literature data the bulk of the nitrogen is found in the diamond cores (Kulakova et al. 2010). Elevated levels of nitrogen on the surface of ND-NH_2 as compared with other samples (Table 1) are due to the presence of amino groups on the surface. It is known that the samples of commercial
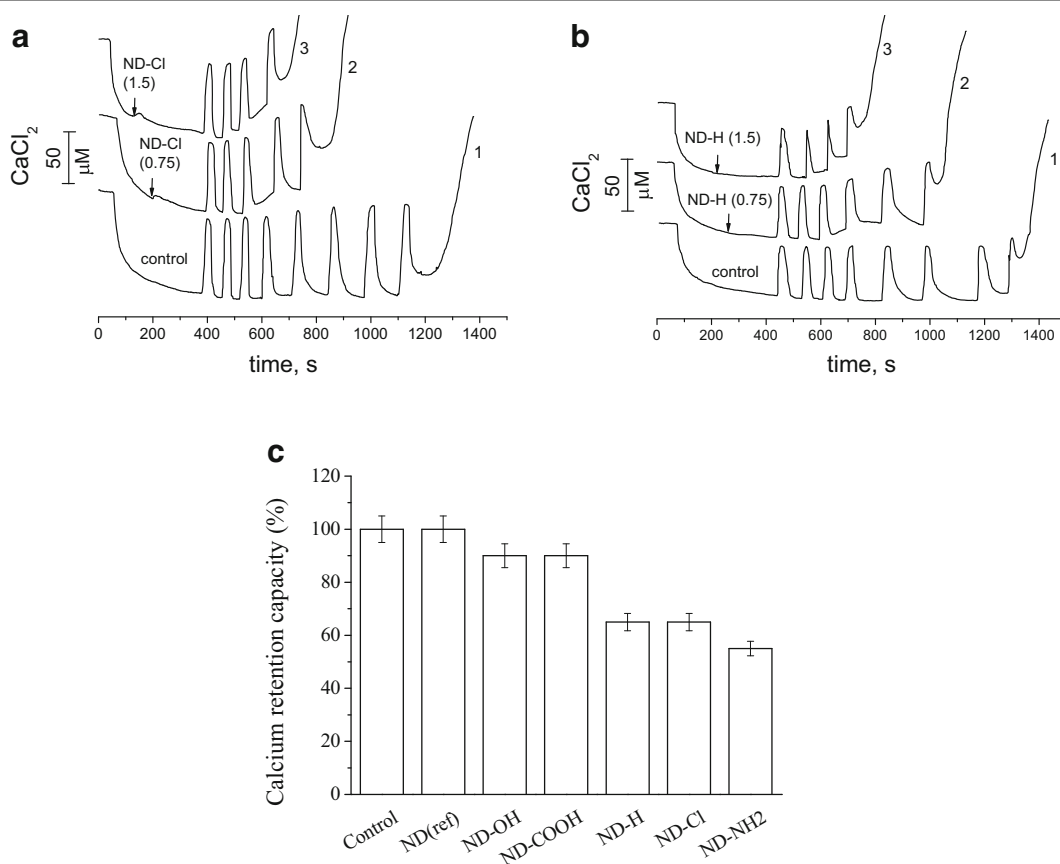
Fig. 7 The effect of modified NDs on the transport of calcium ions in isolated mitochondria. **a** The effect of ND-Cl: control, without the addition of ND (curve 1), in the presence of 0.75 mg/ml (curve 2) and 1.5 mg/ml (curve 3) ND-Cl; **b** the effect of ND-H: control without the addition of ND (curve 1), in the presence of 0.75 mg/ml (curve 2) and 1.5 mg/ml (curve 3) ND-H. Then, each additive of $CaCl_2$ was at a concentration of 25 μM. **c** The comparison of the action of NDs samples with different surface chemistry on the calcium retention capacity of mitochondria. The calcium retention capacity of mitochondria in the control (without additives ND) is adopted 100%. The calcium retention capacity of mitochondria was estimated by the number of absorbed and the cations that were added in the form of $CaCl_2$, in portions of 25 μM. In all experiments, NDs were added at 1.5 mg/ml. 1.2 mg protein of mitochondria was added to 1 ml of incubation medium containing 120 mM KCl, 1.5 mM KH_2PO_4, 10 mM HEPES (pH 7.2), 4 mM glutamate, and 2 mM malate

grade NDs typically contain metal contaminants (Mitev et al. 2013). The chloride ions detected in samples (Fig. 4) may be associated with metal ions comprising the ND impurities, which remain even after further treatment of the original ND.

Thus, analysis of the original ND sample and the functionalized NDs confirms that each of the latter is characterized by an increased content of certain functional groups or atoms: -H on ND-H, -Cl on ND-Cl, -COOH on ND-COOH, -OH on ND-OH, and -NH_2 for ND-NH_2. Furthermore, chlorine atoms are covalently bound with carbon atoms only on the surface of ND-Cl.

The well-known results of biological testing of NDs (Kaur and Badea 2013) emphasize the importance of the

size and concentration of ND particles in ND hydrosols, as well as the chemical nature of the particles surface. In the present work, we prepared hydrosols of functionalized NDs with the same concentration and similar particle size (150–200 nm). Thus, only chemical state of the studied NDs was changed.

All our data indicate that the chemical state of the surface of NDs affects the functional characteristics of mitochondria. For example, samples of ND-Cl and ND-H cause the decrease in mitochondrial membrane potential when potassium pyruvate was used as an oxidation substrate pyruvate (substrate complex I), whereas ND-NH_2, ND-COOH, and ND-OH had no marked effect on the mitochondrial membrane potential. In
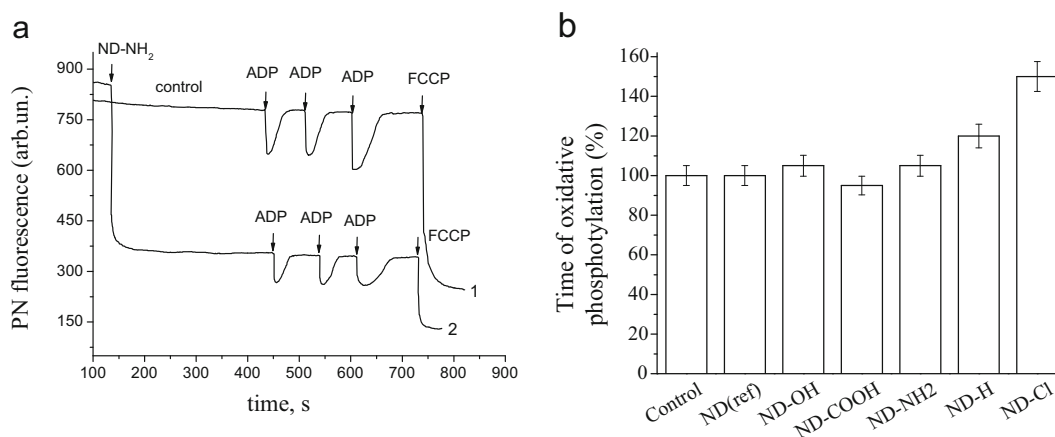
Fig. 8 The effect of NDs on the redox state of the pyridine nucleotides in isolated mitochondria. **a** The original recording of the action of 625 μg/ml ND-NH$_2$ on PN fluorescence. Oxidation/restore of NADH in the oxidative phosphorylation cycle was induced by sequential additions of ADP in concentrations of 200, 400, 800 μm, respectively. The full oxidation of NADH

was initiated by addition of 0.5 μM FCCP. **b** Comparison of the effect of functionalized NDs with different chemical surface on time of oxidative phosphorylation. Time of oxidative phosphorylation cycle of ADP (50 μM) added to the mitochondria in the control (without additives ND) was 50 ± 10 s and taken as 100%

descending order of effect of lowering the mitochondrial membrane potential, functionalized NDs can be listed as follows:

ND-Cl > ND-H > ND-NH$_2$

> ND-OH≥ND(ref)≥ND-COOH.

In the case of using succinate as a substrate of oxidation and blocking complex I by rotenone, all samples of studied NDs caused a decrease in mitochondrial membrane potential. The most active still remained ND-Cl and ND-H, and the least active are ND-COOH and ND(ref).

The effect of changes in mitochondrial membrane potential appeared at sufficiently high concentrations of functionalized NDs: 1.0 mg/ml for ND-Cl and ND-H and 2.5 mg/ml for ND-COOH and ND-OH, correspondingly. This concentration is generally unattainable in the experiments in vivo.

In the earlier cell studies (Sayes et al. 2004), it was shown that the functionalized samples of NDs (hydroxylated, aminated, and carboxylated) administered at the concentration of less than 50 μg/ml had practically no effect on the viability of human embryonic cells HEK 293. Increasing concentration of ND up to 100 μg/ml led to viability reduction to 80% for aminated ND, 90% for hydroxylated ND, and 95% for carboxylated ND, respectively. In the toxicity tests on HeLa cells, it was shown that carboxylated NDs had no toxic effect (at

concentration 100 μg/ml), while NDs modified with (3-aminopropyl)triethoxysilane demonstrated toxic effect (Weng et al. 2012). One of the explanations of the depressive action of ND-Cl and ND-H samples on the membrane potential of mitochondria may be the high hydrophobicity of their surface, which allows these nanoparticles to penetrate more easily into the mitochondrial membrane.

Penetration of NDs into mitochondria with an average diameter of 2–3 nm through the outer membrane channels seems unfeasible, based on the comparison of the sizes of the channel and ND particles. While the primary particle size of ND is ~4–6 nm, NDs form aggregates with an average size of about 150–200 nm. This is much larger than a mitochondrial pore. The fact that the most of the studied NDs samples do not affect the respiratory mitochondrial function, in particular, the redox state of pyridine nucleotides is also in favor of the conclusion that NDs do not penetrate into the mitochondria.

Therefore, a more probable explanation of the ND's effect of reducing the membrane potential is associated with the possible interaction of the particles with transport channels, including mitochondrial pore components, located on the outer mitochondrial membrane.

Indeed, on the basis of obtained data, we can conclude about that the decrease in mitochondrial membrane potential induced by modified NDs leads to opening of a MPTP, and this process is prevented by the inhibitor MPTP CsA (Fig. 6). In this regard, it was

further investigated the influence of the surface chemical composition of NDs on the transport of calcium ions and calcium retention capacity of isolated mitochondria.

It is shown that under conditions of transport and accumulation of calcium ions in mitochondria, NDs induce pores opening at lower concentrations of calcium. Functionalized NDs can be arranged as follows in order to decreasing effect on calcium transport in mitochondria:

$$ND\text{-}NH_2 > ND\text{-}Cl > ND\text{-}H$$
$$> ND\text{-}COOH \approx ND\text{-}OH \geq ND(\text{ref})$$
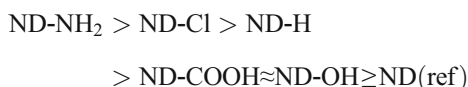
These findings on the impact of the ND(ref) and functionalized ND samples on mitochondrial calcium retention capacity are consistent with the data on their effects on membrane potential with successive addition of NDs to the mitochondria. With the goal of revealing the role of a type of surface groups, difference between samples regarding all other structural factors had been minimized; the studied particles in ND hydrosol samples had almost the same size (150–200 nm), and it was assured that impurities in the samples at the level used in the work do not play a role. Therefore, it can be assumed that the observed difference in mitochondria metabolism upon administration of NDs with different surface groups is mostly based on chemical nature of the surface of the ND samples. The specificity of the effect of certain NDs on the induction of mitochondrial pores has been confirmed by the fact that the original ND did not demonstrate such influence.

From the data of Fig. 8, it is clear that the reduction of the calcium retention capacity is observed upon the incubation of mitochondria with ND-Cl and ND-H, and has a particularly strong effect after incubation with a sample of ND-NH$_2$. Perhaps the activity of the latter is due to the interaction of the amino groups of ND with the components of the mitochondrial pores and the influence on its operation, which is typical, for example, for polyamines (Salvi and Toninello 2004). Educed effect of influence of functionalized NDs on membrane potential and Ca^{2+}-ion transport in the mitochondria suggests that, depending on the chemical nature of the surface, ND induced different mechanisms of its action on these subcellular organelles. This hypothesis can be supported by the conclusion made in the work on the study of the biological activity of quantum dots (Zheng et al. 2017). The authors showed that chemical composition of the surface of nanoparticles, including the nature of the functional groups, is more important in the generation of ROS than surface charge (i.e., zeta potential), whereas surface charge is an important driver of cytotoxicity.

In this regard, there are two important molecular pharmacological aspects of using NDs as drug delivery systems.

The first aspect is more relevant in case of ND as a biomarker or a carrier for delivery of a drug to the tissue/cell, the main (direct) action of which is not associated with mitochondria. In this case, since the ND is able to remain in the cell for a long time (Yakovlev et al. 2014) and even move within the cell (Hayashi et al. 2013), it is important to know how a particular kind of utilized ND would affect the state and energy metabolism of the mitochondria.

A second aspect becomes determining, in case where ND is intended to be used as a delivery vehicle to a cell/organ of a drug, the main effect of which is directly associated with the mitochondria, e.g., antitumor antibiotics (in particular, doxorubicin (Chow et al. 2011), an antioxidant, an analgesic, and others (Smith et al. 2012)). Then, there is the need to consider mechanisms of influence of both the immobilized material, and its carrier-ND on the mitochondria. Depending on the mechanism of involvement drug in direct or indirect mitochondria functioning, ND can enhance or weaken the action of drug on the contrary.

Both effects can be used when creating a new generation of drug delivery systems based on NDs. For example, varying chemical nature of the ND surface, it can be possible to reduce the cytotoxicity of anticancer agents in healthy cells (protective effect). Or, conversely, modification of ND surface groups could be used to increase the effectiveness of antitumor drugs in the target cells, tissues, and organs. It is possible that such an active action of ND surface composition has become a major factor in improving the efficacy of doxorubicin immobilized on ND in vivo experiments with a tumor model, described in detail in previous work (Chow et al., 2011). This only confirms the potential use of ND with an optimized surface (e.g., hydrogenated) as a significant additional factor for the activation of cellular apoptosis through effects on the mitochondria.

Conclusion

This study indicates that using isolated mitochondria is an effective model for a rapid assessment of biological

nonequivalence of ND samples in vitro primarily intended for biomedical applications (Solomatin et al. 2013).

The results also suggest that by selecting specific chemical functionalization of ND (including ND modified with therapeutics), a fine tuning of its specific interactions with mitochondria can be achieved, thus leading to changes in cell bioenergetics. Moreover, since the effect of NDs on mitochondria expresses through specific interactions with membrane pores and channels which have a protein nature, it can be expected that such interactions play a role in other protein structures and receptor-substrate interactions. This mechanism may be crucial to amplification of psychopharmacological and neurological properties of glycine immobilized on ND (Leonidov et al. 2014a, b, c, d, e; Jakovlev et al. 2013).

In conclusion, the functionalized ND can be considered not only as a platform drug delivery system, but also as a fundamentally new active pharmacological agent capable of enhancing or, on the contrary, subsiding the unwanted effect of a particular drug and even lead to the appearance of new pharmacological properties (Leonidov et al. 2014a, b, c, d, e). Directional use of this factor may lead to the development of highly efficient drug delivery systems of a new generation based on functionalized NDs (Jakovlev 2013; Jakovlev et al. 2013; Jakovlev et al. 2015).

Compliance with ethical standards

Conflict of interest The authors declare that they have no conflict of interest.

References

Babcock DF, Herrington J, Goodwin PC, Park YB, Hille B (1997) Mitochondrial participation in the intracellular Ca^{2+} network. J Cell Biol 136(4):833–844. https://doi.org/10.1083/jcb.136.4.833

Balogh PL (ed) (2017) Nanomedicine in cancer. New York: Pan Stanford. ISBN 978-1-315-11436-1 (eBook)

Bottini M, Bruckner S, Nika K, Bottini N, Bellucci S, Magrini A, Bergamaschi A, Mustelin T (2006) Multi-walled carbon nanotubes induce T-lymphocyte apoptosis. Toxicol Lett 160:121–126. https://doi.org/10.1016/j.toxlet.2005.06.020

Chan MS, Liu LS, Leung HM, Lo PK (2017) Cancer-cell-specific mitochondria-targeted drug delivery by dual-ligand-functionalized nanodiamonds circumvent drug resistance. ACS Appl Mater Interfaces 9(13):11780–11789. https://doi.org/10.1021/acsami.6b15954

Chen LB (1988) Mitochondrial membrane potential in living cells. Ann Rev Cell Biol 4:155–181. https://doi.org/10.1146/annurev.cb.04.110188.001103

Chen X, Zhang W (2017) Diamond nanostructures for drug delivery, bioimaging, and biosensing. Chem Soc Rev 46(3):734–760. https://doi.org/10.1039/C6CS00109B

Cheung LTY, Manthey AL, Lai JSM, Chiu K (2017) Targeted delivery of mitochondrial calcium channel regulators: the future of glaucoma treatment? Front Neurosci 11:648. https://doi.org/10.3389/fnins.2017.00648

Chow EK, Zhang X-Q, Chen M, Lam R, Robinson E, Huang H, Schaffer D, Osawa E, Goga A, Ho D (2011) Nanodiamond therapeutic delivery agents mediated enhanced chemoresistant tumor treatment. Sci Trans Med 3(73): 73ra21. https://doi.org/10.1126/scitranslmed.3001713

Danilenko VV (2004) On the history of the discovery of nanodiamond synthesis. Phys Solid State 46:595–599. https://doi.org/10.1134/1.1711431

Denisov SA, Sokolina GA, Spitsyn BV (2010) Effects of amination and adsorption of ammonia on the electrical conductivity of the detonation nanodiamond powders. IOP Conference Series: Materials Science and Engineering IOP Publishing 16(1):012005. https://doi.org/10.1088/1757-899X/16/1/012005

Dolmatov VY (2007) Detonation-synthesis nanodiamonds: synthesis, structure, properties and applications. Rus Chem Rev 76(4):339–360. https://doi.org/10.1070/RC2007v076n04ABEH003643

Dworak N, Wnuk M, Zebrowski J, Bartosz G, Lewinska A (2014) Genotoxic and mutagenic activity of diamond nanoparticles in human peripheral lymphocytes in vitro. Carbon 68:763–776. https://doi.org/10.1016/j.carbon.2013.11.067

Fedotcheva NI, Teplova VV, Fedotcheva TA, Rzheznikov VM, Shimanovskii NL (2009) Effect of progesterone and its synthetic analogues on the activity of mitochondrial permeability transition pore in isolated rat liver mitochondria. Biochem Pharmacol 78:1060–1068. https://doi.org/10.1016/j.bcp.2009.05.028

Fresta CG, Chakraborty A, Wijesinghe MB, Amorini AM, Lazzarino G, Lazzarino G, Tavazzi B, Lunte SM, Caraci F, Dhar P, Caruso G (2018) Non-toxic engineered carbon nanodiamond concentrations induce oxidative/nitrosative stress, imbalance of energy metabolism, and mitochondrial dysfunction in microglial and alveolar basal epithelial cells. Cell Death Dis 9:245. https://doi.org/10.1038/s41419-018-0280-z

Gornall AG, Bardawill CJ, David MM (1949) Determination of serum proteins by means of the biuret reaction. J Biol Chem 177:751–766

Guo C, Wang J, Jing L, Ma R, Liu X, Gao L, Cao L, Duan J, Zhou X, Li Y, Sun Z (2018) Mitochondrial dysfunction, perturbations of mitochondrial dynamics and biogenesis involved in

endothelial injury induced by silica nanoparticles. Environ Pollut 236:926–936. https://doi.org/10.1016/j.envpol.2017.10.060

Halliwell B (1991) Reactive oxygen species in living systems: source, biochemistry, and role in human disease. Am J Med 91(3C):14S–22S. https://doi.org/10.1016/0002-9343(91)90279-7

Hayashi K, Pack CG, Sato MK, Mouri K, Kaizu K, Takahashi K, Okada Y (2013) Viscosity and drag force involved in organelle transport: investigation of the fluctuation dissipation theorem. Eur Phys J E 36:136. https://doi.org/10.1140/epje/i2013-13136-6

Hens SC, Cunningham G, Tyler T, Moseenkov S, Kuznetsov V, Shenderova O (2008) Nanodiamond bioconjugate probes and their collection by electrophoresis. Diam Relat Mater 17:1858–1866. https://doi.org/10.1016/j.diamond.2008.03.020

Ho D, Wang C-HK, Chow EK-H (2015) Nanodiamonds: the intersection of nanotechnology, drug development, and personalized medicine. Sci Adv 1(7):e1500439. https://doi.org/10.1126/sciadv.1500439

Hong G, Diao S, Antaris AL, Dai H (2015) Carbon nanomaterials for biological imaging and nanomedicinal therapy. Chem Rev 115(19):10816–10906. https://doi.org/10.1021/acs.chemrev.5b00008

Jakovlev RJ (2013) Nano-diamond conjugate with glycine and method for producing said conjugate. EP 2662080,

Jakovlev RJ, Leonidov NB, Gubanok AI. (2013) Antibacterial agent and method for preparing it. RU Pat 2476215.

Jakovlev RJ, Rodina EV, Valueva AV, Vorob'eva NN, Lisichkin GV, Leonidov NB (2015) Conjugate of nanodiamond with pyrophosphatase and method of obtaining thereof. RU Pat 2542411.

Jia G, Wang H, Yan L, Wang X, Pei R, Yan T, Zhao Y, Guo X (2005) Cytotoxicity of carbon nanomaterials: single-wall nanotube, multi-wall nanotube, and fullerene. Environ Sci Technol 39:1378–1383. https://doi.org/10.1021/es048729l

Johnson D, Lardy HA (1967) Isolation of liver or kidney mitochondria. Methods Enzymol 10:94–96. https://doi.org/10.1016/0076-6879(67)10018-9

Kamo N, Muratsugu M, Hongoh R, Kobatake Y (1979) Membrane potential of mitochondria measured with an electrode sensitive to tetraphenyl phosphonium and relationship between proton electrochemical potential and phosphorylation potential in steady state. J Membr Biol 49(2):105–121. https://doi.org/10.1007/BF01868720

Karpukhin AV, Avkhacheva NV, Yakovlev RY, Kulakova II, Yashin VA, Lisichkin GV, Safronova VG (2011) Effect of detonation nanodiamonds on phagocyte activity. Cell Biol Int 35:727–733. https://doi.org/10.1042/CBI20100548

Kaur R, Badea I (2013) Nanodiamonds as novel nanomaterials for biomedical applications: drug delivery and imaging systems. Int J Nanomedicine 8:203–220. https://doi.org/10.2147/IJN.S37348

Keremidarska M, Ganeva A, Mitev D, Hikov T, Presker R, Pramatarova L, Krasteva N (2014) Comparative study of cytotoxicity of detonation nanodiamond particles with an osteosarcoma cell line and primary mesenchymal stem cells. Biotechnol Biotechnol Equip 28(4):733–739. https://doi.org/10.1080/13102818.2014.947704

Kondrashova MN, Fedotcheva NI, Saakyan IR, Sirota TV, Lyamzaev KG, Kulikova MV, Temnov AV (2001) Preservation of native properties of mitochondria in rat liver homogenate. Mitochondrion 1:249–267. https://doi.org/10.1016/S1567-7249(01)00025-3

Korolkov VV, Kulakova II, Tarasevich BN, Lisichkin GV (2007) Dual reaction capacity of hydrogenated nanodiamond. Diam Relat Mater 16(12):2129–2132. https://doi.org/10.1016/j.diamond.2007.07.018

Kulakova II (2004) Surface chemistry of nanodiamonds. Phys Solid State 46(4):636–643. https://doi.org/10.1134/1.1711440

Kulakova II, Korol'kov VV, Yakovlev RY, Lisichkin GV (2010) The structure of chemically modified detonation-synthesized nanodiamond particles. Nanotechnol Russ 5(7–8):474–485. https://doi.org/10.1134/S1995078010070074

Kumari SH, Singh MK, Singh SK, Grácio JJA, Dash D (2013) Nanodiamonds activate blood platelets and induce thromboembolism. Nanomedicine 9(3):427–440. https://doi.org/10.2217/nnm.13.23

Lai L, Li YP, Mei P, Chen W, Jiang FL, Liu Y (2016) Size effects on the interaction of QDs with the mitochondrial membrane in vitro. J Membr Biol 249(6):757–767

Leonidov NB, Jakovlev RJ, Kulakova IV, Lisichkin GV (2014a) Antihypooxant and method for preparing it. RU Pat 2506074

Leonidov NB, Jakovlev RJ, Kulakova IV, Lisichkin GV (2014b) Anxiolytic and method for preparing it. RU Pat 2519755

Leonidov NB, Jakovlev RJ, Lisichkin GV (2014c) Antipsychotic agent and method for preparing it. RU Pat 2519761

Leonidov NB, Jakovlev RJ, Lisichkin GV (2014d) Agent with anti-stroke action and method for preparing it. RU Pat 2521404

Leonidov NB, Jakovlev RJ, Solomatin AS, Lisichkin GV (2014e) Antidepressant drug and method for preparing it. RU Pat 2519759

Lisichkin GV, Korol kov VV, Tarasevich BN, Kulakova II, Karpukhin AV (2006) Photochemical chlorination of nanodiamond and interaction of its modified surface with C-nucleophiles. Russ Chem Bull (Int Ed) 55(12):2212–2219. https://doi.org/10.1007/s11172-006-0574-7

Lisichkin GV, Kulakova II, Gerasimov YA, Karpukhin AV, Yakovlev RY (2009) Halogenation of detonation-synthesised nanodiamond surfaces. Mendeleev Commun 19:309–310. https://doi.org/10.1016/j.mencom.2009.11.004

Magrez A, Kasas S, Salicio V, Pasquier N, Seo JW, Celio M, Catsicas S, Schwaller B, Forro L (2006) Cellular toxicity of carbon-based nanomaterials. Nano Lett 6(6):1121–1125. https://doi.org/10.1021/nl060162e

Mendes RG, Bachmatiuk A, Buchner B, Cuniberti G, Rummeli MH (2013) Carbon nanostructures as multi-functional drug delivery platforms. J Mater Chem B 1:401–428. https://doi.org/10.1039/C2TB00085G

Mitev DP, Townsend AT, Paull B, Nesterenko PN (2013) Direct sector field ICP-MS determination of metal impurities in detonation nanodiamond. Carbon 60:326–334. https://doi.org/10.1016/j.carbon.2013.04.045

Mitev DP, Townsend AT, Paull B, Nesterenko PN (2014) Screening of elemental impurities in commercial detonation nanodiamond using sector field inductively coupled plasma-mass spectrometry. J Mater Sci 49:3573–3591. https://doi.org/10.1007/s10853-014-8036-3

Mkandawire M, Pohl A, Gubarevich T, Lapina V, Appelhans D, Rodel G, Pompe W, Shreiber J, Opitz J (2009) Selective

targeting of green fluorescent nanodiamond conjugates to mitochondria in HeLa cells. J Biofoton 2(10):596–606. https://doi.org/10.1002/jbio.200910002

Munnich A, Rustin P (2001) Clinical and diagnosis of mitochondrial disorders. Am J Med Genet 106(1):4–17. https://doi.org/10.1002/ajmg.1391

Mytych J, Wnuka M, Rattan SIS (2016) Low doses of nanodiamonds and silica nanoparticles have beneficial hormetic effects in normal human skin fibroblasts in culture. Chemosphere 148:307–315. https://doi.org/10.1016/j.chemosphere.2016.01.045

Naserzadeh P, Esfeh FA, Kaviani M, Ashtari K, Kheirbakhsh R, Salimi A, Pourahmad J (2018) Single-walled carbon nanotube, multi-walled carbon nanotube and Fe_2O_3 nanoparticles induced mitochondria mediated apoptosis in melanoma cells. Cutan Ocul Toxicol 37(2):157–166. https://doi.org/10.1080/15569527.2017.1363227

Nebel CE, Rezek B, Shin D, UetsukaH YN (2007) Diamond for bio-sensor applications. J Phys D 40(20):6443–6466. https://doi.org/10.1088/0022-3727/40/20/S21

Nutt LK, Pataer A, Pahler J, Fang B, Roth J, McConkey DJ, Swisher SG (2002) Bax and Bak promote apoptosis by modulating endoplasmic reticular and mitochondrial Ca^{2+} stores. J Biol Chem 277(11):9219–9225. https://doi.org/10.1074/jbc.M106817200

Pathak Y, Thassu D. (eds.) (2016). Drug delivery nanoparticles formulation and characterization (Vol. 191). CRC Press

Salvi M, Toninello A (2004) Effects of polyamines on mitochondrial Ca^{2+} transport. Biochim Biophys Acta 1661:113–124. https://doi.org/10.1016/j.bbamem.2003.12.005

Sayes CM, Fortner JD, Guo W, Lyon D, Boyd AM, Ausman KD, Tao YJ, Sitharaman B, Wilson LJ, Hughes JB, West JL, Colvin VL (2004) The differential cytotoxicicty of water-soluble fullerenes. Nano Lett 4(10):1881–1887. https://doi.org/10.1021/nl0489586

Schafer FQ, Buettner GR (2001) Redox environment of the cell as viewed through the redox state of the glutathione disulfide/glutathione couple. Free Radic Biol Med 30(11):1191–1212. https://doi.org/10.1016/S0891-5849(01)00480-4

Schrand AM, Huang H, Carlson C, Schlager JJ, Osawa E, Hussain SM, Dai L (2007) Are diamond nanoparticles cytotoxic? J Phys Chem B 111(1):2–7. https://doi.org/10.1021/jp066387v

Shenderova OA, Gruen DM (eds.) (2006) Ultrananocrystalline diamond: synthesis, properties, and applications. New York: William Andrew Publ. Norwich

Shugalei IV, Voznyakovskii AP, Garabadzhiu AV, Tselinskii IV, Sudarikov AM, Ilyushin MA (2013) Biological activity of detonation nanodiamond and prospects in its medical and biological applications. Russ J Gen Chem 83(5):851–883. https://doi.org/10.1134/S1070363213050010

Smith RAJ, Hartley RC, Cocheme HM, Murphy MP (2012) Mitochondrial pharmacology. Trends Pharmacol Sci 33(6): 341–350. https://doi.org/10.1016/j.tips.2012.03.010

Solomatin AS, Yakovlev RY, Fedotcheva NI, Kondrachova MN, Leonidov NB (2013) Method of determining biological inequivalence of nanodiamonds. RU Pat 2538611

Szewczyk A, Wojtczak L (2002) Mitochondria as a pharmacological target. Pharmacol Rev 54(1):101–127. https://doi.org/10.1124/pr.54.1.101

Thomas V, Halloran BA, Ambalavanan N, Catledge SA, Vohra YK (2012) In vitro studies on the effect of particle size on macrophage responses to nanodiamond wear debris. Acta Biomater 8(5):1939–1947. https://doi.org/10.1016/j.actbio.2012.01.033

Turrens JF (2003) Mitochondrial formation of reactive oxygen species. J Physiol 552(Pt 2):335–344. https://doi.org/10.1113/jphysiol.2003.049478

Wehling J, Dringen R, Zare RN, Maas M, Rezwan K (2014) Bactericidal activity of partially oxidized nanodiamonds. ACS Nano 8(6):6475–6483. https://doi.org/10.1021/nn502230m

Weng MF, Chang BJ, Chiang SY, Wang NS, Niu H (2012) Cellular uptake and phototoxicity of surface-modified fluorescent nanodiamonds. Diam Relat Mater 22:96–104. https://doi.org/10.1016/j.diamond.2011.12.035

Whitlow J, Pacelli S, Paul A (2017) Multifunctional nanodiamonds in regenerative medicine: recent advances and future directions. J Control Release 261:62–86. https://doi.org/10.1016/j.jconrel.2017.05.033

Wong BS, Yoong SL, Jagusiak A, Panczyk T, Ho HK, Ang WH, Pastorin G (2013) Carbon nanotubes for delivery of small molecule drugs. Adv Drug Deliv Rev 65(15):1964–2015. https://doi.org/10.1016/j.addr.2013.08.005

Yakovlev RY, Osipova OS, Solomatin AS, Kulakova II, Muravyova GP, Avramenko NV, Leonidov NB, Lisichkin GV (2015) An approach to unification of the physicochemical properties of commercial detonation nanodiamonds. Russ J Gen Chem 85(6):1565–1574. https://doi.org/10.1134/S1070363215060365

Yakovlev RY, Solomatin AS, Leonidov NB, Kulakova II, Lisichkin GV (2014) Detonation diamond—a perspective carrier for drug delivery systems. Russ J Gen Chem 84(2): 379–390. https://doi.org/10.1134/S1070363214020406

Zhang X, Hu W, Li J, Tao L, Wei Y (2012) A comparative study of cellular uptake and cytotoxicity of multi-walled carbon nanotubes, graphene oxide, and nanodiamond. Toxicol Res 1:62–68. https://doi.org/10.1039/C2TX20006F

Zhao X, Ren X, Zhu R, Luo Z, Ren B (2016) Zinc oxide nanoparticles induce oxidative DNA damage and ROS-triggered mitochondria-mediated apoptosis in zebrafish embryos. Aquat Toxicol 180:56–70. https://doi.org/10.1016/j.aquatox.2016.09.013

Zheng H, Mortensen LJ, Ravichandran S, Bentley K, DeLouise LA (2017) Effect of nanoparticle surface coating on cell toxicity and mitochondria uptake. J Biomed Nanotechnol 13(2):155–166. https://doi.org/10.1166/jbn.2017.2337